

High temperature electrolyzer based on solid oxide co-ionic electrolyte: A theoretical model

Anatoly Demin^{a,*}, Elena Gorbova^a, Panagiotis Tsiakaras^b

^a Institute of High Temperature Electrochemistry, 22 S. Kovalevskoy, 620219 Yekaterinburg, Russia

^b School of Engineering, Department of Mechanical Engineering, University of Thessaly, Pedion Areos, 383 34 Volos, Greece

Received 7 September 2006; received in revised form 11 January 2007; accepted 13 January 2007

Available online 20 January 2007

Abstract

In the present work a theoretical model of a solid oxide electrolyzer based on an electrolyte having both oxygen ion and proton conductivity is considered. The main parameters of the electrolytic process and an electrolyzer (distribution of gas components, electromotive forces and current densities along the electrolyzer channel, average values of electromotive forces and current densities) were calculated depending on a proton transport number and mode of the reactants' feeding (co- and counter-flow). The performed analysis demonstrates considerable influence of the mode of feeding on all parameters of the electrolyzer: operation under the counter-flow mode is preferable as regards the specific characteristics and uniformity of their distribution along the electrolyzer. It is shown that the electrolyzer's specific characteristics increase with the increase of the proton transport number.

© 2007 Elsevier B.V. All rights reserved.

Keywords: Solid oxide electrolyzer; Co-ionic electrolyte; High temperature steam electrolysis

1. Introduction

Hydrogen production by means of water electrolysis is a very attractive way for pure hydrogen production by using electrical energy during a period when using the electricity by other consumers is minimal. Advanced low temperature electrolyzers demonstrate rather low power inputs, about 4.1 kWh/m³ H₂, which corresponds to an average cell voltage of 1.71 V.

An idea to use electrochemical devices based on solid oxides for hydrogen production by means of steam decomposition appeared in the late 1960s [1]. In the late 1970s Rohr [2] performed series of experiments with electrolysis cells and stacks and showed that they have acceptable stability during ca. 8000 h. Since then the base of the electrolysis cells was yttria-stabilized zirconia (YSZ) having oxygen ion conductivity. It was demonstrated that a high temperature solid oxide electrolyzer (SOE) based on an oxygen ion solid oxide electrolyte had acceptable characteristics when it worked at 1.1 V [3], which corresponded

to electrical power inputs 2.63 kWh/m³ H₂. In this case it is necessary to supply the SOE electrochemical section and the vaporizer with additional heat (about 0.5 kWh/m³ H₂ each), but both electrical power inputs and total (electrical + heat) inputs are significantly lower than in the low temperature electrolyzer.

In the beginning of 1980s, oxides having proton conductivity were discovered and at the very early stage it was proposed to use them for steam electrolysis [4,5]. Since then a number of experiments were performed with the cells based on protonic electrolytes (see, for instance, [6,7]). Recently, the interest to the application of protonic electrolytes for steam electrolyzers is growing [8,9].

It is known now that only a little part of "protonic electrolytes" has practically pure proton conductivity. A great number of these solid oxides possess a significant part of oxygen ion conductivity in addition to proton conductivity, so it is logical to call them "co-ionic electrolyte" [10]. It was shown that an achievable efficiency of a solid oxide fuel cell (SOFC) increases, as the proton transport number of the electrolyte increases [11]. However the most known proton electrolytes are unstable in CO₂-containing atmosphere which is typical to the SOFC. The problem of carbonates formation is absent in the SOE for steam splitting, so it is possible to use a co-ionic electrolyte in the SOE. It is interesting

Abbreviations: SOE, solid oxide electrolyzer; SOFC, solid oxide fuel cell

* Corresponding author. Fax: +7 3432 745 992.

E-mail address: a.demin@ihte.uran.ru (A. Demin).

Nomenclature	
a	anode
c	cathode
E	electromotive force
F	Faraday constant
h	electrolyte thickness
H	enthalpy
i	current density
I	current
j	mass flux
K	equilibrium constant of the reaction of hydrogen oxidation
L	length of the channel-working zone
p	dimensionless partial pressure; heat flux
R	gas constant
t	transport number
T	absolute temperature
U	voltage
x	coordinate of the channel working zone
X	component of the gas mixture
<i>Greek letter</i>	
σ	conductivity
<i>Subscripts</i>	
eff	effective value
F	related to Faraday process
H	related to proton transport
H ₂	hydrogen
H ₂ O	steam
O	related to oxygen ion transport
O ₂	oxygen
th	thermoneutral
tot	total
T	absolute temperature
ν	related to convective mass transport

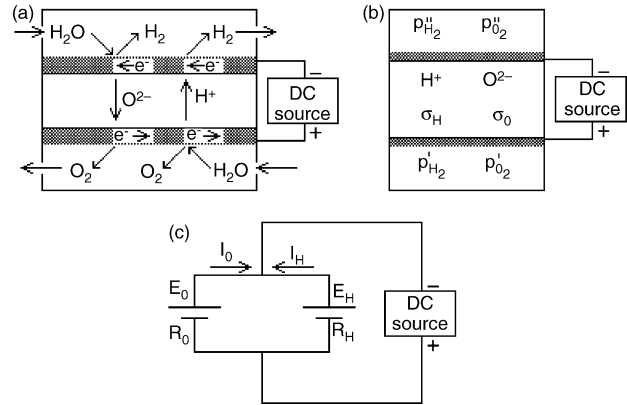


Fig. 1. A schematic diagram of the processes in the SOE based on a co-ionic electrolyte (a); an electrolytic cell based on a co-ionic electrolyte (b); an equivalent circuit of the cell (c).

At the cathode, decomposition of water occurs as follows:



Protons move across the electrolyte to the anode where they form hydrogen:



So, reactions (1) and (3) are two ways for hydrogen formation at the anode of the SOE. Oxygen ions forming at the cathode according to the reaction (1) move to the cathode where they form oxygen:



This reaction and the reaction (2) are mechanisms of oxygen formation in the SOE.

From the electrochemical point of view, the SOE presents an ionic conductor opposite sides of which are in contact with different gas atmospheres (Fig. 1b). The electrolyte has two types of charge carriers, namely, oxygen ions and protons and can be characterized by corresponding conductivities, σ_{O} and σ_{H} . Each gas phase can be characterized by the dimensionless partial pressures of oxygen, hydrogen and steam, p_{O_2} , p_{H_2} and $p_{\text{H}_2\text{O}}$, respectively. The first two values are equal to the corresponding mole fractions of the components if they are mixed with steam; in case they are chemically bonded, the corresponding partial pressures are calculated by using the following equations:

$$p_{\text{O}_2} = \left(\frac{p_{\text{H}_2\text{O}}}{K p_{\text{H}_2}} \right)^2 \quad (5)$$

$$p_{\text{H}_2} = \frac{p_{\text{H}_2\text{O}}}{K p_{\text{O}_2}^{1/2}} \quad (6)$$

where K is the equilibrium constant of the reaction of hydrogen oxidation.

An equivalent circuit of the SOE based on the co-ionic electrolyte presents two parallel galvanic cells connected with an external current source (Fig. 1c). Each galvanic cell is due to presence of the given charge carrier and is characterized by an electromotive force, EMF, due to drop of corresponding partial

from theoretical point of view to analyze the influence of ion transport numbers on the SOE characteristics.

2. Theoretical model

A simplified scheme of the processes occurring in the SOE based on the co-ionic electrolyte is presented in Fig. 1a. The SOE consists of the electrolyte membrane opposite sides of which are in contact with porous electrodes, an anode and a cathode, which, in turn, are in contact with gas flows moving within corresponding gas channels. The electrodes are connected with a DC power source. In general case, steam is fed to both the cathode and anode channel.

At the anode, water is decomposed to hydrogen and oxygen ions according the following electrochemical reaction:



pressure, and by an internal resistance to transfer of corresponding charge carrier. The electromotive forces are calculated by the following equations:

$$E_O = -\frac{RT}{4F} \ln \frac{p''_{O_2}}{p'_{O_2}} \quad (7)$$

$$E_H = \frac{RT}{2F} \ln \frac{p'_{H_2}}{p''_{H_2}} \quad (8)$$

where R , T , F are the ideal gas constant, absolute temperature and Faraday's constant, respectively. The resistances are calculated as follows:

$$R_O = \frac{R}{t_O} \quad (9)$$

$$R_H = \frac{R}{t_H} \quad (10)$$

where t_O , t_H are transport numbers of oxygen ions and protons, respectively, determined as follows:

$$t_O = \frac{\sigma_O}{\sigma} \quad (11)$$

$$t_H = \frac{\sigma_H}{\sigma} \quad (12)$$

In the frame of this consideration, it is assumed that resistances of the electrochemical reactions (1)–(4) are negligible as compared with the resistances for ions transfer (9) and (10).

Applying laws of electrical circuits to the circuit of Fig. 1c partial currents connected with transport of corresponding ions, I_O and I_H can be calculated. It is more convenient to use values of current densities, i_O and i_H , which can be presented by the following equations:

$$i_O = \frac{\sigma t_O (U - E_O)}{h} \quad (13)$$

$$i_H = \frac{\sigma t_H (U - E_H)}{h} \quad (14)$$

where h is the electrolyte thickness. Combination of Eqs. (13) and (14) gives the total ion current density, i_{tot} .

$$i_{tot} = \frac{\sigma (U - E_{eff})}{h} \quad (15)$$

where

$$E_{eff} = t_O E_O + t_H E_H \quad (16)$$

is an effective electromotive force of the cell based on the co-ionic electrolyte.

Fluxes of the components from (to) the electrodes due to reactions (1)–(4), called Faraday fluxes, j_F , are equal

$$j_{F,H_2} = \frac{i_O + i_H}{2F} \quad (17)$$

$$j_{F,H_2O}(c) = -\frac{i_O}{2F} \quad (18)$$

at the cathode and:

$$j_{F,O_2} = \frac{i_O + i_H}{4F} \quad (19)$$

$$j_{F,H_2O}(a) = -\frac{i_H}{2F} \quad (20)$$

at the anode; minus means disappearance of the component.

Gas mixtures moving along the channels can be characterized by convective fluxes of the components, j_{v,O_2} , j_{v,H_2} , $j_{v,H_2O}(c)$, $j_{v,H_2O}(a)$, and by total fluxes, $j_v(c)$ and $j_v(a)$, for the cathode and for the anode channels, respectively. It is obvious that the ratio of the convective flux value of a given component to the total convective flux value for a given cross-section of the channel just equal to the partial pressure of the component in this cross-section. Change of the convective fluxes along the channels due to the Faraday fluxes obeys to equations:

$$\frac{dj_{v,H_2}}{dx} = j_{F,H_2} \quad (21)$$

$$\frac{dj_{v,O_2}}{dx} = j_{F,O_2} \quad (22)$$

$$\frac{dj_{v,H_2O}(c)}{dx} = j_{F,H_2O}(c) \quad (23)$$

$$\frac{dj_{v,H_2O}(a)}{dx} = j_{F,H_2O}(a) \quad (24)$$

The following SOE characteristics were calculated: relative fluxes of steam at the inlet of the cathode and anode channels; distributions of partial pressures of the components, EMF values and partial current densities along the SOE; average values of EMFs and partial current densities within the SOE. Each set of data was calculated for a number of the proton transport number.

The following algorithm was used for the calculations. The length of the working part of the SOE was set as 1. It was divided into great number of intervals (up to 2000). Chosen values of partial pressures of the components in the input and output gases were assigned. Initial values of inlet convective fluxes to the anode and to the cathode channels were assigned as a first approximation. From the parameters of the inlet gas mixtures, values of EMFs and partial current densities in the initial point were calculated using Eqs. (7) and (8) and Eqs. (13) and (14), respectively. By using Eqs. (13) and (14) and Eqs. (17)–(24), changes of convective fluxes of each component X within the first interval were calculated according to the following equation:

$$\Delta j_{v,X} = j_{F,X} \Delta x \quad (25)$$

Values of the components' convective fluxes at the end of the first interval were calculated and then EMFs and partial current densities in this point were also calculated. Afterwards, the procedure was repeated for the next interval, and again right to the end of the channel. Obtained partial pressures of the components in the outlet gases were compared with the chosen assigned values; in case they differ from each other the initial values of the inlet convective fluxes were corrected and the calculations were repeated from the beginning. The cycles of the calculations were repeated until close agreement between the obtained and

the assigned partial pressures of the component was achieved. The calculations were performed in the shell Delphi 6.0.

In order to reveal the main peculiarities of the SOE based on a co-ionic electrolyte, the following parameters were assigned. The inlet cathode gas: $\text{H}_2\text{O} + \text{H}_2$, $p_{\text{H}_2\text{O}} = 0.98$; the inlet anode gas: $\text{H}_2\text{O} + \text{O}_2$, $p_{\text{H}_2\text{O}} = 0.995$; the outlet cathode gas: $\text{H}_2 + \text{H}_2\text{O}$, $p_{\text{H}_2\text{O}} = 0.1$; the outlet anode gas: $\text{O}_2 + \text{H}_2\text{O}$, $p_{\text{H}_2\text{O}} = 0.1$; $T = 1100 \text{ K}$; modes of gas feeding: co-flow and counter-flow; applied voltage: 1.1 V; electrolyte specific conductivity: $\sigma/h = 1 \text{ Smcm}^{-2}$. The latter parameter is real for supporting electrolyte; its value does not influence the distribution of gas components' concentrations and EMFs along the channels. The presented current densities are called "conditional current densities", i.e., corresponding to the condition $\sigma/h = 1 \text{ Smcm}^{-2}$. The obtained results for the current densities can be easily recalculated for other values σ/h . The range of the proton transport number was chosen from 0.02 to 0.98.

3. Results and discussion

It is clear that the input steam flows to the cathode and anode channels depend on the proton transport number: the higher t_{H} value the less the steam flow to the cathode channel; on the contrary, the anode steam flow increases with the t_{H} value increase. It was found that for a given t_{H} value the inlet flows both to the cathode and anode channel practically do not depend on the mode of reagents' feeding. The cathode input flow decreases practically linearly with the t_{H} value increase. It is illustrated in Fig. 2 where the input flows are presented in relative values: they are referred to the unit of produced hydrogen. The anode input flow demonstrates also practically linear increasing with the t_{H} value increase.

The results on distributions of the cell characteristics are presented for dimensionless relative cell length, x/L , where x is the current coordinate of the cell, L is the cell length. It is assumed that the point $x = 0$ corresponds to the cathode inlet.

Figs. 3 and 4 illustrate the distributions of the partial pressures of the electrolysis products, hydrogen and oxygen, along the channels for three cases: (i) the electrolyte has practically pure

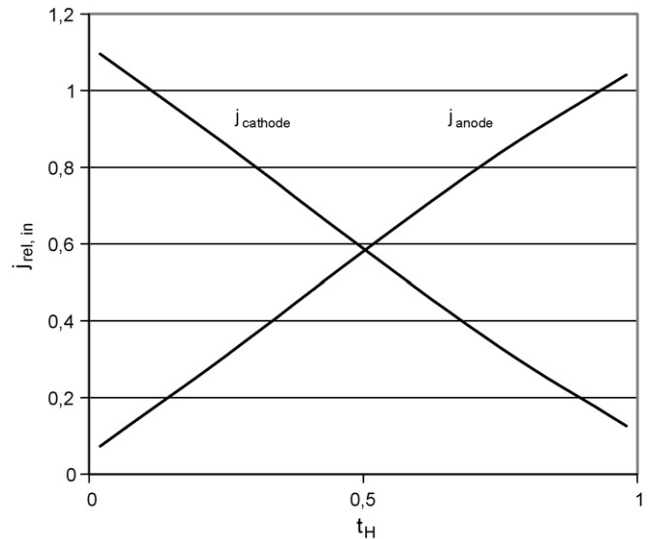


Fig. 2. Dependence of the relative input steam flows on the proton transport number.

oxygen conductivity ($t_{\text{H}} = 0.02$), (ii) partial conductivities are equal ($t_{\text{H}} = 0.5$) and (iii) the conductivity is practically protonic ($t_{\text{H}} = 0.98$). One can see that both the mode of reagents' supply and the proton transport number value influence the distribution. The difference of oxygen partial pressures distributions for the co- and counter-flow modes is quite obvious first of all due to opposite directions of the anode flows. However, it is easy to see that the distributions are not symmetrical.

The proton transport number value also influences strongly the distributions of the components in the channels. Rapid increase of the oxygen partial pressure at the initial part of the anode channel at $t_{\text{H}} = 0.02$ is connected with the predominant transport of oxygen through the electrolyte into the anode compartment where oxygen is mixed with the small steam flow. On the contrary, at $t_{\text{H}} = 0.98$ the steam flow is many times bigger and the oxygen partial pressure rises slowly (Fig. 3, left). The difference in the rate of the change of the hydrogen partial pressure depending on the t_{H} value can be explained analogically. The

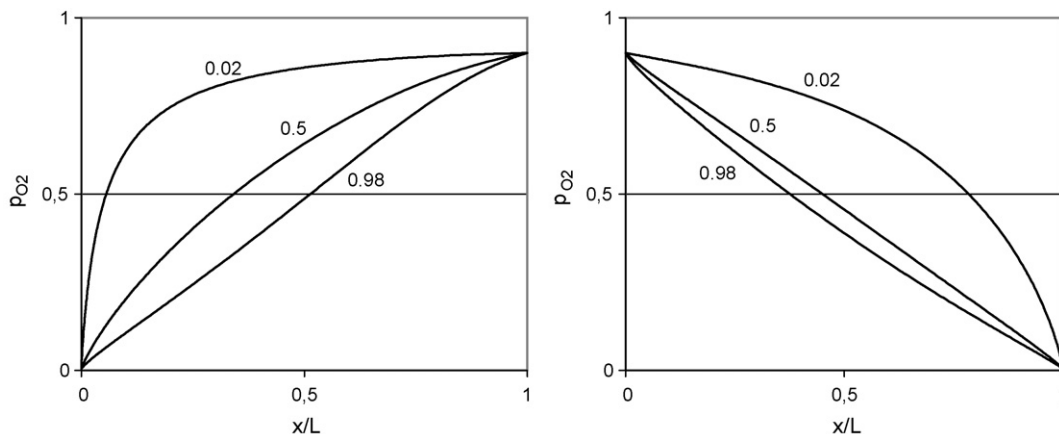


Fig. 3. Distribution of the oxygen partial pressure along the SOE for the co-flow (left) and counter-flow (right) modes. Number at the lines denotes proton transport number.

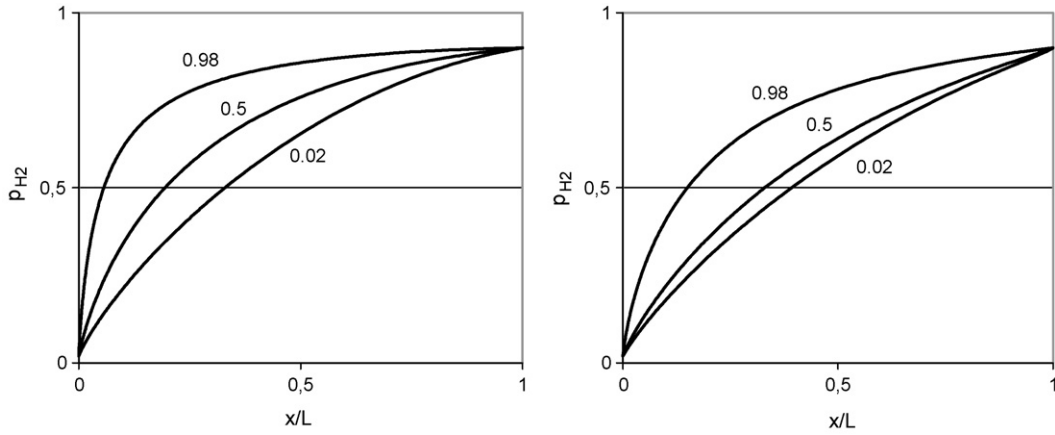


Fig. 4. The same as in Fig. 3 for the hydrogen partial pressure.

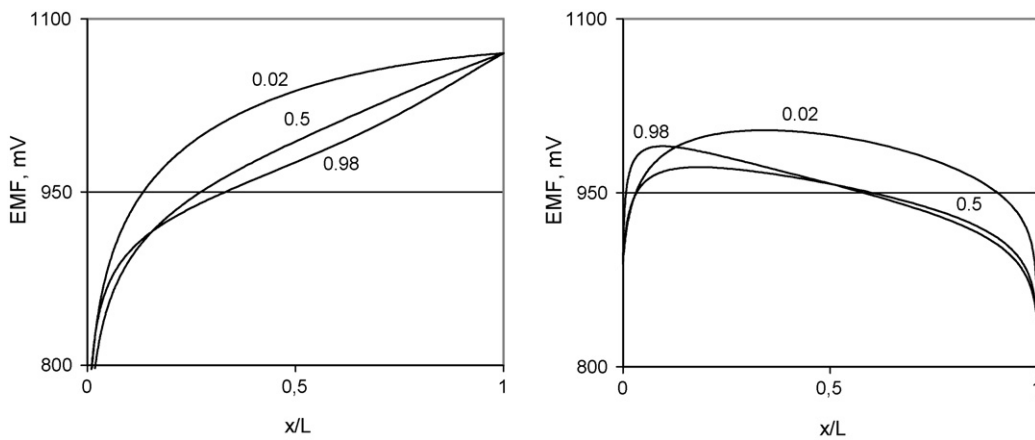


Fig. 5. Distribution of E_H along the SOE under co-flow (left) and counter-flow (right) mode. Number at the lines denotes proton transport number.

distributions of the components in the channels allow finding EMFs' distributions.

Figs. 5 and 6 show distributions of E_H and E_O , respectively, for both modes of reagents' supply. The most remarkable features are several ones. First, under the counter-flow mode, both E_H and E_O are lower on average than under the co-flow mode. Second, under the counter-flow mode, distributions of both E_H and E_O are more uniform than under the co-flow mode. Third,

under the co-flow mode, both E_H and E_O change monotonously with the t_H value increases, the former increases and the latter decreases. On the contrary, under the counter-flow mode, both E_H and E_O have evident minimum at some intermediate values of t_H .

In Figs. 7 and 8 are shown the distributions of the conditional partial current densities along the SOE for the proton and oxygen ion charges, respectively. It can be distinguished that

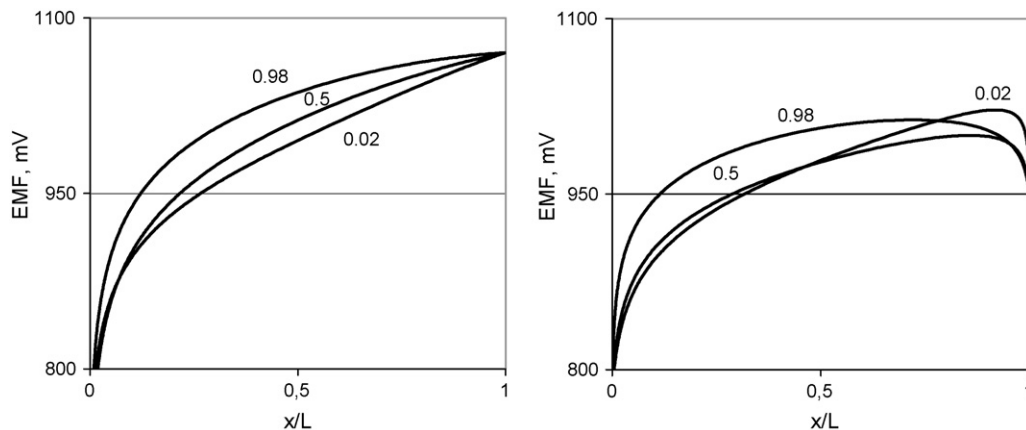


Fig. 6. The same as in Fig. 4 for E_O .

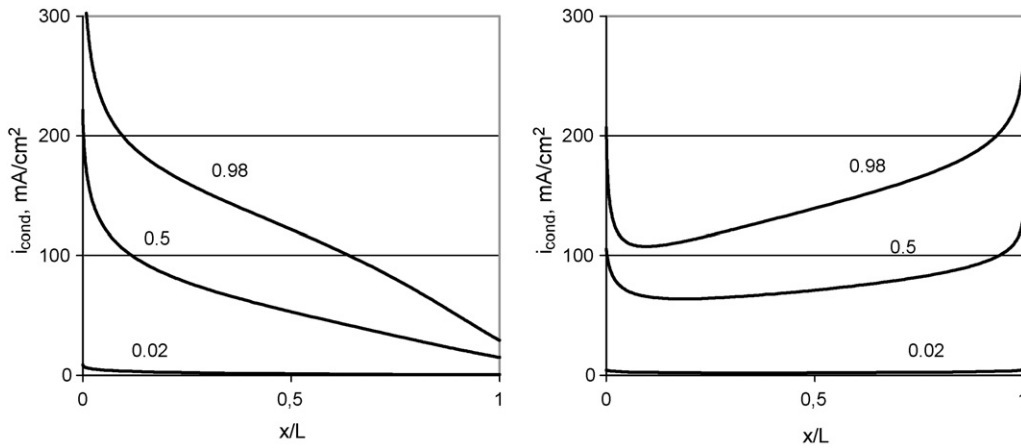


Fig. 7. Distribution of the conditional proton current density along the SOE under co-flow (left) and counter-flow (right) mode. Number at the lines denotes proton transport number.

under the counter-flow mode, both the proton and the oxygen ion current densities are more uniform and slightly higher than under the co-flow mode. The obtained results are of the great importance for the calculations of the partial convective flows of the reagents and products in both the anode and the cathode channels. Besides, they allow calculating the distribution of heat flux, p_Q , along the SOE by using equation:

$$p_Q = i_{\text{tot}}(U - U_{\text{th},T}) \quad (26)$$

where $U_{\text{th},T}$ is thermoneutral voltage determined as:

$$U_{\text{th},T} = \frac{-\Delta H_T}{2F} \quad (27)$$

where ΔH_T is the enthalpy change of the hydrogen oxidation reaction at temperature T . In the frame of this work the distribution of the heat flux was not calculated. However, the main conclusion is obvious: the heat flux distribution is more uniform under the counter-flow mode; hence temperature distribution in the SOE in this case must also be more uniform.

The advantages of the counter-flow mode of the reagents' supply as well as the use of the co-ionic electrolyte with higher t_H value become more obvious when analyzing Fig. 9. The most important characteristic for the SOE on the whole is the average

effective EMF value which can be found by numerical integration of the E_O and E_H distributions and using Eq. (16). It is interesting that under the co-flow mode, the average effective EMF has a maximum at $t_H \approx 0.3$ whereas the average effective EMF is minimal at $t_H \approx 1$ under the counter-flow mode. This means that the region of $t_H \approx 0.3$ is unfavourable for the co-flow mode of operation because in this case the generated current density is minimum. For both modes of operation, the proton electrolyte demonstrates the minimum average effective EMF and, hence, the maximum total current density can be achieved.

Fig. 10 confirms the said above. Presented here are the average values of the partial and total current densities obtained by numerical integration of the current densities distributions depending on the proton transport number. On the whole, the average value of the total current density is visibly higher under the counter-flow than under the co-flow mode. It is necessary to point out that the difference increases with the decrease of the applied voltage that can be achieved in thin-film design of the SOE. The value σ/h for thin-film systems can be significantly higher. For instance, according to [12] the value $\sigma/h \approx 10 \text{ S cm}^{-2}$. If such electrolyte will be used in the SOE then the average current can reach 0.95 A cm^{-2} under counter-flow

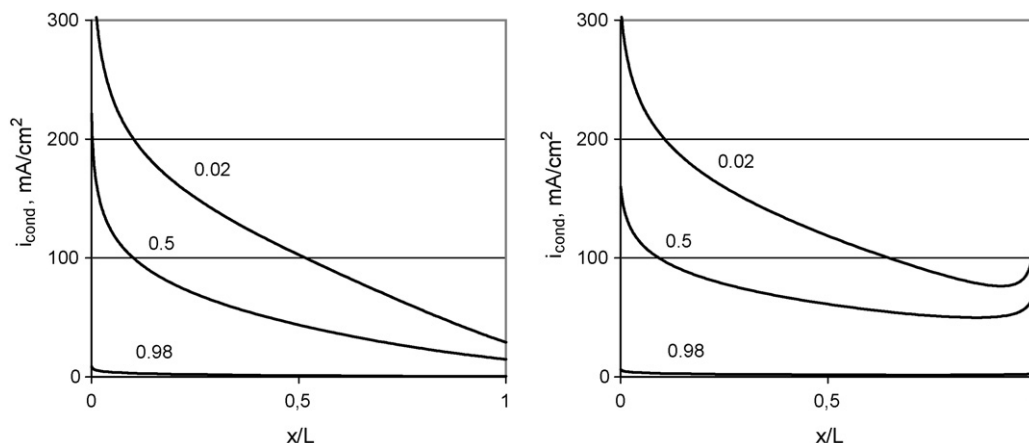


Fig. 8. The same as in Fig. 6 for the oxygen ion current density.

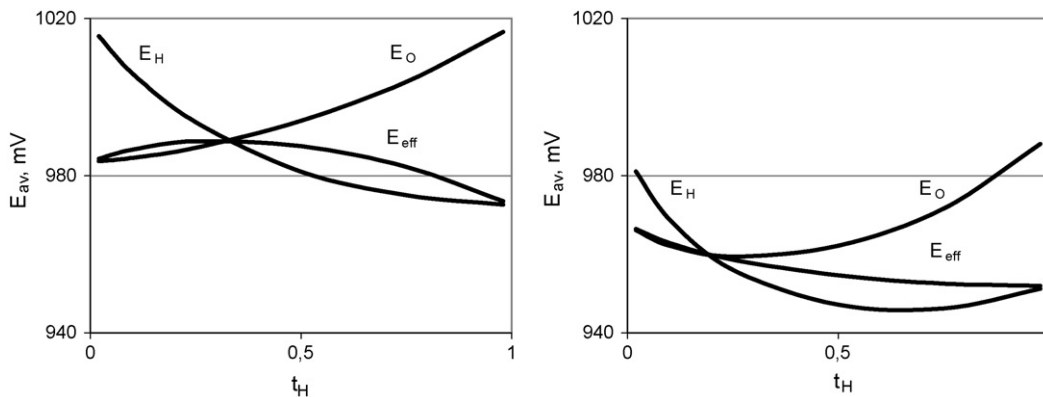


Fig. 9. Dependence of the average EMFs on the proton transport number under co-flow (left) and counter-flow (right) mode.

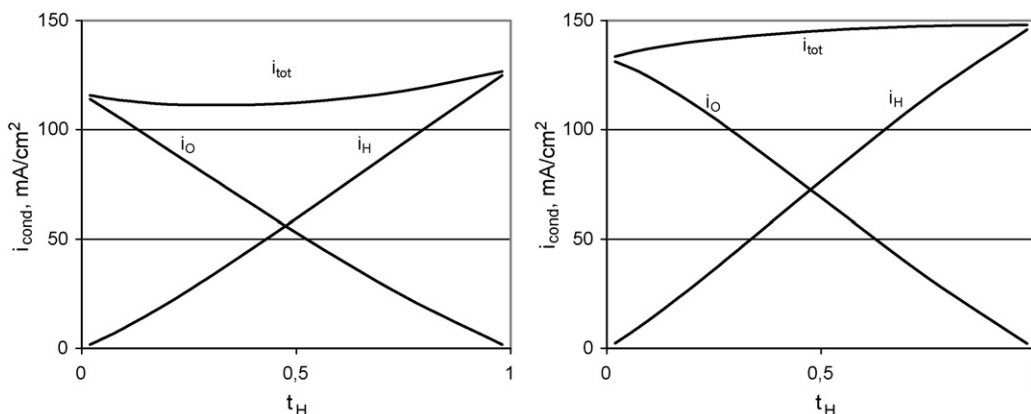


Fig. 10. Dependence of the average partial and total conditional current densities on the proton transport number under co-flow (left) and counter-flow (right) mode.

mode and 0.6 A cm^{-2} under co-flow mode under the applied voltage $U = 1.05 \text{ V}$.

4. Conclusion

The performed analysis shows that the co-ionic electrolyte can be successfully utilized as a base of solid oxide electrolyzer. One of interesting distinctions of this electrolyzer from the one based on the oxygen ion electrolyte is the mode of feeding by steam: the latter must be fed to both the anode and cathode channels, the part of the cathode feeding being higher with t_H increasing. Another interesting peculiarity of the electrolyzer based on the co-ionic electrolyte is more uniform distributions of its specific characteristics (current density and specific heat flow rate) under the counter-flow mode of feeding. It is interesting also that the average current density is visibly higher when the SOE operates under the counter-flow mode comparing to operation under the co-flow mode, the difference being higher with the applied voltage decreasing.

The most promising application of the SOE is its utilization for hydrogen production when it is supplied by electrical energy in combination with high potential heat for heating the electrochemical section and with low potential heat for heating the vaporizer. The mentioned heat can be supplied from a nuclear power station or from a concentrator of solar energy. In this case,

the considerable part of expensive electrical energy is replaced by cheap heat energy; this is impossible for low temperature electrolyzers. The SOE based on the co-ionic electrolyte has higher specific characteristics comparing to the SOE based on the oxygen ion electrolyte. This is a base either for increase of the SOE efficiency under the same size of the unit, or for decrease of the unit size under the same efficiency. So, utilization of the co-ionic electrolyte in the SOE is very prospect and development of the co-ionic electrolytes is very actual.

References

- [1] H.S. Spacil, J.T. Tedmon, J. Electrochem. Soc. 116 (1969) 1618.
- [2] F. J. Rohr, in: T., Takahashi, A., Kozawa, (Eds.), Applications of Solid Electrolytes, JEC Press, Cleveland, OH, p. 196.
- [3] A.K. Demin, B.L. Kuzin, A.S. Lipilin, Soviet Electrochim. 23 (1987) 1258.
- [4] H. Iwahara, T. Esaka, H. Uchida, N. Maeda, Solid State Ionics 3/4 (1981) 359.
- [5] H. Iwahara, H. Uchida, N. Maeda, J. Power Sources 7 (1982) 293.
- [6] H. Iwahara, Solid State Ionics 52 (1992) 99.
- [7] H. Iwahara, Solid State Ionics 77 (1995) 289.
- [8] T. Schober, Solid State Ionics 162/163 (2003) 277.
- [9] J.W. Phair, S.P.S. Badwal, Ionics 12 (2006) 103 (Water electrolysis for H_2).
- [10] N. Arestova, V. Gorelov, Russ. J. Electrochem. 30 (1994) 892–894.
- [11] A. Demin, P. Tsiakaras, Int. J. Hydrogen Energ. 26 (2001) 1103–1108.
- [12] Ya. Mizutani, K. Hisada, K. Ukai, H. Sumi, M. Yokoyama, Ya. Nakamura, O. Yakamoto, J. Alloys Compd. 408–412 (2006) 518–524.